

The triangular-lattice Hubbard model: a frustrated highly correlated electron system

This article has been downloaded from IOPscience. Please scroll down to see the full text article.

1994 J. Phys.: Condens. Matter 6 L625

(<http://iopscience.iop.org/0953-8984/6/41/001>)

View [the table of contents for this issue](#), or go to the [journal homepage](#) for more

Download details:

IP Address: 171.66.16.151

The article was downloaded on 12/05/2010 at 20:44

Please note that [terms and conditions apply](#).

LETTER TO THE EDITOR

The triangular-lattice Hubbard model: a frustrated highly correlated electron system

C J Gazza, A E Trumper, and H A Ceccatto

Instituto de Física Rosario, Universidad Nacional de Rosario, Bvd. 27 de Febrero 210 Bis, 2000 Rosario, Argentina

Received 8 July 1994

Abstract. We have studied the ground-state properties of the half-filled Hubbard model on the triangular lattice by means of the slave-boson technique. The combined effects of high correlation and frustration in this non-bipartite lattice produce a rich phase diagram, including paramagnetic, commensurate spiral, and linear spin-density-wave phases, as well as a metal-insulator transition. Unlike previous Hartree–Fock studies of this model, the slave-boson technique predicts no metallic incommensurate spiral state to be the stable ground state in any region of parameter space.

In recent years there has been an upsurge of interest in highly correlated electron systems, particularly in its prototype, the Hubbard model [1]. Related problems, like the metal–insulator transition [2] and the properties of slightly doped quantum antiferromagnets, have also received intense scrutiny. This has been motivated by the proposals of new superconducting mechanisms based on the electron–electron correlation [3], in order to explain the high critical temperatures observed in the ceramic compounds. For this reason, most of the studies have focused on the Hubbard model on the square lattice, particularly in the strong repulsion (large- U) limit. At half filling this system is an antiferromagnetic insulator for all values of U due to the perfect nesting of the non-interacting Fermi surface. Interesting features in the ground-state magnetic properties, like incommensurate spiral structures, appear only off half filling [4, 5, 6]. On the other hand, on non-bipartite lattices as the triangular one, even for the half-filled case the Hubbard model has a very rich ground-state structure [9, 10], including a paramagnetic phase, different magnetic long-range orders, and a metal–insulator transition. The triangular lattice has served in the past as a playground for novel ideas on unconventional phases of frustrated antiferromagnets [7]. The so called RVB state, and the concomitant concept of ‘spin liquid’, have been devised as possible ground states produced by the inherent frustration in this geometry. These ideas have been recently recycled into some of the above mentioned proposals to explain the physics of the Cu–O planes [8].

All the physics described above originates in the combined effects of strong correlation and frustration. These effects appear naturally tied together in the Hubbard model on the triangular lattice

$$H = -t \sum_{i,\delta,\sigma} c_{i\sigma}^\dagger c_{i+\delta,\sigma} + U \sum_i n_{i\uparrow} n_{i\downarrow} \quad (1)$$

where i indicates lattice sites, and δ represent the vectors pointing to the six nearest neighbours of a given site. This model has been previously studied in [9, 10] using the Hartree–Fock approximation. In this work we reexamine its ground-state properties by

means of the rotational-invariant slave-boson approach as developed in [11]. Consequently, we write the spinor $\mathbf{c}_i \equiv (c_{i\uparrow}, c_{i\downarrow})$ as $\mathbf{c}_i = Z_i \mathbf{f}_i$. Here Z_i is a 2×2 boson matrix that describes the background (site-occupation) changes when fermions move, and the pseudofermion spinor $\mathbf{f}_i \equiv (f_{i\uparrow}, f_{i\downarrow})$ takes care of the Fermi statistics in the hopping processes (see [11] for the definition of Z_i and other details). Under rotations these operators will transform as $\mathbf{f}_i \rightarrow \psi \mathbf{f}_i$ and $Z_i \rightarrow \psi Z_i \psi^\dagger$ respectively, where ψ is a $SU(2)$ matrix. Now, to describe spiral magnetic structures with wavevector \mathbf{Q} it is convenient to transform to a local reference frame with its z axis pointing in the direction of the local magnetization. In this twisted frame the entries of the boson matrices Z_i can be replaced by site-independent numbers as usual. Then, for spirals around the y axis the Hamiltonian (1) is changed to

$$H'_{\text{Sb}} \equiv H_{\text{Sb}} - \mu \sum_i \mathbf{f}_i^\dagger \cdot \mathbf{f}_i = N H_0 - \sum_{i,\delta} \mathbf{f}_i^\dagger A(\delta) \mathbf{f}_{i+\delta} - \sum_i \mathbf{f}_i^\dagger B \mathbf{f}_i \quad (2)$$

where N is the number of lattice sites. The matrix

$$A(\delta) \equiv t Z^\dagger \psi_i^\dagger \psi_{i+\delta} Z = t \begin{pmatrix} \alpha_\uparrow^2 \cos \frac{Q \cdot \delta}{2} & \alpha_\uparrow \alpha_\downarrow \sin \frac{Q \cdot \delta}{2} \\ -\alpha_\uparrow \alpha_\downarrow \sin \frac{Q \cdot \delta}{2} & \alpha_\downarrow^2 \cos \frac{Q \cdot \delta}{2} \end{pmatrix}$$

where $\alpha_\uparrow, \alpha_\downarrow$ are defined below, and $B = (\lambda_0^{(2)} + \mu) \tau_0 + \lambda^{(2)} \cdot \boldsymbol{\tau}$. Here τ_0 is the 2×2 identity matrix and $\boldsymbol{\tau}$ the vector of Pauli matrices. The four $\lambda^{(2)}$ s are Lagrange multipliers that impose the equivalence in computing the mean particle and (vector) spin densities using either Z or \mathbf{f}_i . In the twisted reference frame there is no transversal spin components, so that we can take $\lambda_1^{(2)} = 0 = \lambda_2^{(2)}$, and Z becomes diagonal: $Z_{\sigma\sigma'} = \alpha_\sigma \delta_{\sigma\sigma'}$. The diagonal elements are given by

$$\alpha_\sigma = \frac{1}{\sqrt{(1-d^2-p_\sigma^2)}} (e p_\sigma + d p_{-\sigma}) \frac{1}{\sqrt{(1-e^2-p_{-\sigma}^2)}}$$

where $e^2, p_\uparrow^2, p_\downarrow^2$, and d^2 are, respectively, the site probabilities of having a hole, a single electron (polarized parallel or antiparallel to the local z axis), and double occupancy. The constant $H_0 = U d^2 - \lambda^{(1)}(e^2 + p_\uparrow^2 + p_\downarrow^2 + d^2 - 1) + \lambda_0^{(2)}(p_\uparrow^2 + p_\downarrow^2 + 2d^2) + \lambda_3^{(2)}(p_\uparrow^2 - p_\downarrow^2)$. The Lagrange multiplier $\lambda^{(1)}$ takes care that the mean occupation probabilities add up to one, which ensures, on average, the physical size for the bosonic sector of state space.

The diagonalization in momentum space of the effective fermion Hamiltonian (2) gives the dispersion relations

$$\epsilon_\sigma(\mathbf{k}) = \frac{(A_{\mathbf{k}, \uparrow} + A_{\mathbf{k}, \downarrow})}{2} + \sigma \sqrt{\left(\frac{A_{\mathbf{k}, \uparrow} - A_{\mathbf{k}, \downarrow}}{2} \right)^2 + B_{\mathbf{k}}^2} \quad (\sigma = \pm).$$

We defined

$$A_{\mathbf{k}, \sigma} = t \alpha_\sigma^2 \gamma_{\mathbf{k}}^c + \lambda_0^{(2)} + \sigma \lambda_3^{(2)} \quad B_{\mathbf{k}} = t \gamma_{\mathbf{k}}^s \alpha_\uparrow \alpha_\downarrow$$

where

$$\gamma_{\mathbf{k}}^c = \frac{1}{2} \sum_{\delta, \sigma} \cos(\mathbf{k} + \sigma \mathbf{Q}/2) \cdot \delta \quad \gamma_{\mathbf{k}}^s = \frac{1}{2} \sum_{\delta, \sigma} \sigma \cos(\mathbf{k} + \sigma \mathbf{Q}/2) \cdot \delta.$$

The minimization of the ground-state energy with respect to $\lambda_0^{(2)}, \lambda_3^{(2)}, \lambda^{(1)}, e, p_\sigma$ and d produces seven consistency equations that are solved numerically. We used an iterative method which requires, at every step, adjusting the chemical potential μ to fix the particle density $n = 1$, and determining the corresponding Fermi surface. These calculations are performed for different values of \mathbf{Q} , in order to find the proper ground-state magnetic

structure as a function of U . To allow a precise determination of the Fermi surface, in the paramagnetic and spiral phases we solved the problem using a 800×800 grid to cover the Brillouin zone. In the gapped antiferromagnetic phase we used the Gauss–Legendre integration method with 120×120 points. We checked that these approximations produce no detectable error in the curves shown.

Before presenting the results obtained by using the slave-boson approach, we will briefly discuss the picture that emerges from the Hartree–Fock approximation [9]. (We have reobtained these results without using the ‘spinon’ and ‘holon’ picture of Krishnamurthy *et al.*) At $T = 0$, for small values of U/t the system is a paramagnetic metal. At $U_{P \rightarrow Sp} \simeq 3.98t$ there is a transition into an incommensurate spiral semimetallic state. If only spiral magnetic states are considered, at a higher value $U_{Sp \rightarrow AF} \simeq 5.27t$ there is a first-order transition from the spiral metal into an insulator. The insulating state has the three-sublattice order of the classical triangular antiferromagnet, with magnetic wavevector $Q_0 = (4\pi/3a, 0)$. In the region between $U_{P \rightarrow Sp}$ and $U_{Sp \rightarrow AF}$ the wavevector Q changes continuously with U , from $Q_1 \simeq 0.58Q_0$ at $U_{P \rightarrow Sp}$ to $Q_2 \simeq 0.88Q_0$ at $U_{Sp \rightarrow AF}$.

Exactly at this point there is a sudden jump to $Q_0 = (4\pi/3a, 0)$, corresponding to the commensurate-spiral three-sublattice antiferromagnet.

In figure 1 we show the ground-state energy *per site* as a function of U . For the sake of comparison we present both the slave-boson and Hartree–Fock results. As expected, there is *no much difference between the predictions for the magnetic phases, while the energy of the paramagnetic metal is considerably lower in the slave-boson approach*. In fact, the energy gain in this region washes up the possibility of having incommensurate spiral states as in the Hartree–Fock phase diagram. According to the slave-boson approach the system goes from the paramagnetic phase directly into the antiferromagnetic insulator via a first-order transition at $U_{P \rightarrow AF} \simeq 7.23t$ (figure 1(a)).

Incommensurate magnetic structures appear only as metastable states according to this approximation (figure 1(b)). If the paramagnetic phase is continued into the antiferromagnetic stability region, like in the square-lattice case there is a Mott transition at $U_{Mott} = 8|\epsilon_0| = 15.813$, where ϵ_0 is the triangular-lattice tight-binding energy.

In a further work [10] Jayaprakash *et al* have considered the possibility that a linear spin density wave (SDW) could compete in energy with spiral states. They found that a commensurate linear SDW with ordering at wavevector $Q = (\pi/a, 0)$ intervenes between the spiral and the antiferromagnetic states. At $U_{Sp \rightarrow L} \simeq 4.45t$ the spiral SDW with $Q \simeq 0.66Q_0$ becomes unstable and the system goes, via a first-order transition, into a semiconducting state with the magnetization polarized linearly. This state is the ground state for $U_{Sp \rightarrow L} < U < U_{L \rightarrow AF} \simeq 6.2t$. At this point there is a new first-order transition to the three-sublattice antiferromagnetic phase. The linear SDW state becomes favourable against the spiral structures because of the zigzagging ferromagnetic pathways that this order presents (figure 2). These pathways contribute to lower the kinetic energy, which, for the mentioned range of U , overcomes the loose in magnetic energy with respect to the spiral order. It seems plausible that this mechanism could stabilize the linear SDW phase in the slave-boson approach too. We have looked for solutions to the consistency equations corresponding to site occupations having the symmetry shown in figure 2. These calculations are more demanding since now one has to diagonalize a 4×4 matrix at every k point. In this case we used a 200×200 grid to cover the Brillouin zone of the decorated rectangular lattice. We found that for a small range $U_{P \rightarrow L} \simeq 6.9t < U < U_{L \rightarrow AF} \simeq 7.8t$ the linear SDW becomes the ground-state (figure 3). Notice that this state has lower energy than the paramagnetic solution because of its magnetic structure, and better energy than the antiferromagnetic order because of its kinetic energy. As shown in the inset to figure 3, the linear SDW somehow

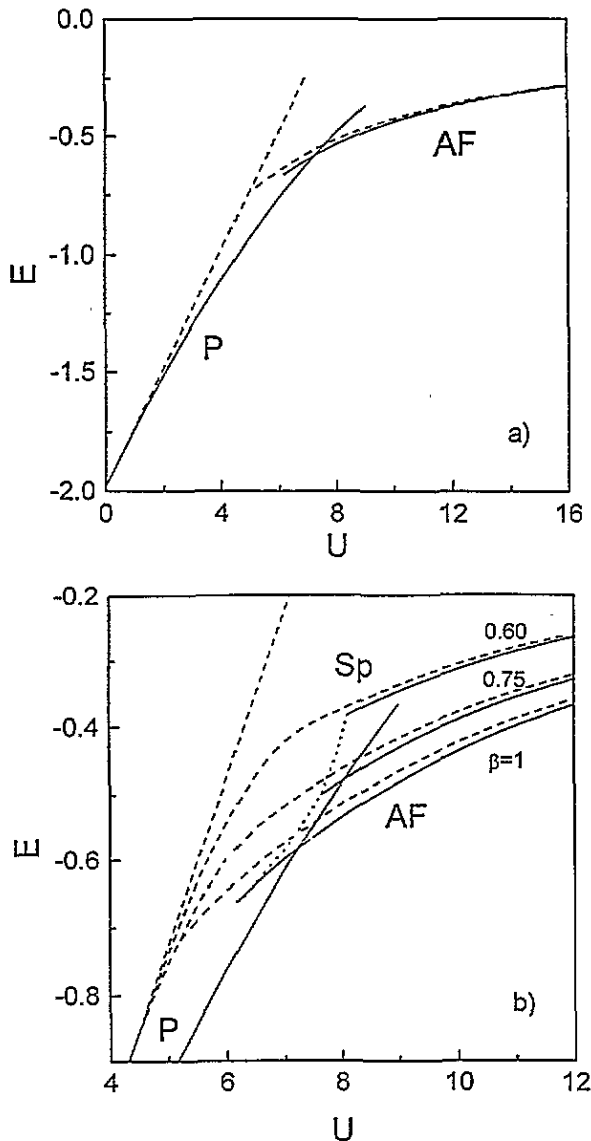


Figure 1. Ground-state energy E as a function of the on-site repulsion U . Full lines are slave-boson results; dashed lines correspond to the Hartree-Fock predictions. (a) P: paramagnetic solution; AF: antiferromagnetic solution with magnetic wavevector $Q_0 = (4\pi/3a, 0)$. (b) Sp: incommensurate spiral solutions with magnetic wavevectors βQ_0 , for $\beta = 0.60$ and 0.75 . The dotted line gives the points at which a gap opens up in the spiral solutions.

interpolates between these two phases. Furthermore, in agreement with the Hartree-Fock prediction, [10] this state is semiconducting in its stability region. In conclusion, we have applied the rotational-invariant slave-boson approach to the study of the half-filled triangular-lattice Hubbard model. For increasing values of U the ground state presents a metallic paramagnetic phase, a semimetallic commensurate linear SDW phase, and the classical three-sublattice antiferromagnetic phase. Furthermore, unlike the Hartree-Fock approximation,

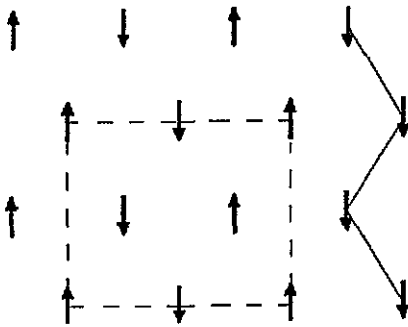


Figure 2. The magnetization pattern in the commensurate linear spin-density-wave state. The dashed line shows the four-site unit cell. Notice the zigzagging ferromagnetic pathways.

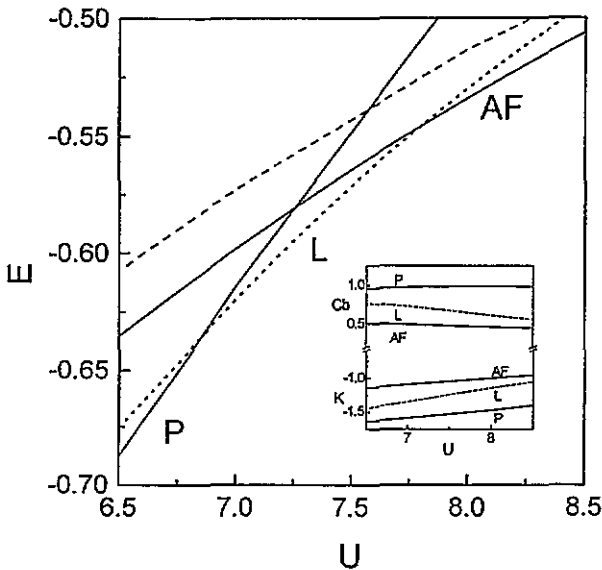


Figure 3. Ground-state energy E as a function of U . P: paramagnetic solution; AF: antiferromagnetic solution; L: linear spin-density-wave state. The dashed line is the Hartree-Fock antiferromagnetic solution. Inset: kinetic (K) and Coulomb (Cb) energies in the various phases.

the slave-boson technique predicts that metallic incommensurate spiral structures never become stable. The prediction of spiral phases by the Hartree-Fock approximation seems to be due only to its poor treatment of the paramagnetic metal. Conversely, it could be argued that the slave-boson approach probably lowers too much the energy of this phase, specially because of the *ad hoc* denominators required to recover the $U = 0$ limit. [11] Other more reliable approximations are required to settle this question. Finally, we mention that the absence of particle-hole symmetry makes interesting to extend this study off half filling. The non-bipartite nature of the lattice would then show up as differences in the doping with

particles or holes. This study is however very time-consuming from a computational point of view, so it is deferred to a future publication.

One of the authors (HAC) is grateful to Fundación Antorchas for partial financial support.

References

- [1] Hubbard J 1963 *Proc. Roy. Soc. London A* **276** 238; 1964 **281** 401
- [2] Mott N F 1974 *Metal Insulator Transitions* (London: Taylor and Francis)
- [3] Rice T M 1987 *Z. Phys. B* **67** 141
- [4] Shraiman B I and Siggia E D 1989 *Phys. Rev. Lett.* **62** 1564
- [5] Schultz H J 1990 *Phys. Rev. Lett.* **64** 1445
- [6] Frésard R Dzierzawa M and Wölfle P 1991 *Europhys. Lett.* **15** 325;
Frésard R and Wölfle P 1992 *J. Phys.: Condens. Matter* **4** 3625
- [7] Anderson P W 1973 *Mater. Res. Bull.* **8** 153
- [8] Anderson P W 1987 *Science* **235** 1196
- [9] Krishnamurthy H R, Jayaprakash C, Sarker S and Wenzel W 1990 *Phys. Rev. Lett.* **64** 950
- [10] Jayaprakash C, Krishnamurthy H R, Sarker S and Wenzel W 1991 *Europhys. Lett.* **15** 625
- [11] Li T, Wölfle P and Hirschfeld P J 1989 *Phys. Rev. B* **40** 6817;
Frésard R and Wölfle P 1992 *Int. J. Mod. Phys. B* **6** 685